

Multilayered coatings with alternate ZrN and TiAlN superlattices

D. J. Li,^{a)} M. Cao, and X. Y. Deng

College of Physics and Electronic Information Science, Tianjin Normal University, Tianjin 300074, China

X. Sun

Department of Mechanical and Materials Engineering, University of Western Ontario, London, Ontario N6A 5B9, Canada

W. H. Chang and W. M. Lau

Surface Science Western, University of Western Ontario, London, Ontario N6A 5B7, Canada

(Received 15 November 2007; accepted 29 November 2007; published online 19 December 2007)

ZrN/TiAlN multilayers with various modulation periods and ratios were grown by ion beam assisted deposition. The nanoscale multilayered modulation was confirmed by Auger electron spectroscopy. All multilayers possess higher hardness than the rule-of-mixture value of monolithic coatings. These properties critically depend on both modulation period and ratio. The multilayer with modulation period of 6.5 nm and ratio of 2:3 displays the highest hardness (>30 GPa) and critical fracture load (53.3 mN). These improvements in properties are likely the result of nanoscale strain optimization as the evolution of layer crystallinity finally reaches the formation of (111) textures in all layers. © 2007 American Institute of Physics. [DOI: 10.1063/1.2826284]

ZrN is an interesting and versatile material owing to its low electrical resistivity, good corrosion resistance, low formation energy, high mechanical properties, and warm golden color.¹⁻³ In comparison, although TiAlN also exhibits high chemical, thermal, and mechanical stabilities, its application is basically in the field of wear-resistant tool coatings.⁴ Typically, ZrN and TiAlN possessing the best mechanical properties are deposited by physical vapor deposition.⁵⁻¹¹ However, thin films thus prepared commonly suffer from the undesirable nature of compressive stress accumulation with the increase in the film thickness that leads to brittle fracture, delamination, and plastic deformation. Recent advanced thin film research has clearly shown that nanoscale strain optimization by engineering multilayers with various compositions, modulation periods, and modulation ratios, is an effective way to overcome this problem and to create new materials possessing desirable properties far superior to those of the constituents in the multilayers.

The aim of this work is to deposit nanoscale ZrN/TiAlN multilayered coatings with different modulation periods (Λ) and modulation ratios, i.e., thickness ratio ($t_{\text{ZrN}}:t_{\text{TiAlN}}$), using our ion beam assisted deposition (IBAD) system. Our purpose is to obtain some insight into the relation between the layered structure and properties of the coatings.

Our IBAD system has two ion sources, one rotatable water-cooled sample holder, and one rotatable water-cooled target holder. The description of the IBAD system can be found in our previous article.⁹ Before deposition, silicon (100) wafer substrates were cleaned with 500 eV Ar⁺ sputtering. The introduction of Ar and N₂ flows to the two ion sources were independently controlled using the mass-flow controllers. The Zr and Ti_{0.5}Al_{0.5} targets were sputtered alternately by Ar⁺ at 1.4 keV to supply Zr or TiAl to the sample surface; simultaneously the surface was also bombarded by N⁺ at 100 eV from the second ion source to synthesize ZrN/TiAlN multilayers. The base pressure was better than 3×10^{-4} Pa, and working pressure was about 2×10^{-2} Pa.

In this work, we used the surface sensitive technique of Auger electron spectroscopy (AES) with a PHI model P660 SAM system to measure elemental compositions and depth profiles of the coatings. In these measurements, a 5 keV electron beam was used to excite Auger electron emission from the sample surface. For depth profiling, an Ar⁺ ion beam at 3 keV with a raster area of 4.0×4.0 mm² was employed. Samples were tilted 30° from normal beam incidence toward the Ar⁺ ion gun. A D/MAX 2500 diffractometer was used for crystallinity analysis, and the measurements were carried out at 40 kV and 40 mA, with Cu K α radiation at 1.540 56 Å. The residual stress of the coatings was measured using an XP-2 profiler. A Nano Indenter XP system was employed to perform hardness and elastic modulus tests. In these tests, the continuous stiffness measurement technique was adopted, a technique which allows the continuous measurement of the contact stiffness during loading. The scratch scan recorded the scratch depth during scratching.

A series of ZrN/TiAlN multilayers with different Λ and constant $t_{\text{ZrN}}:t_{\text{TiAlN}}$ of 2:3 were synthesized. The AES depth profiles of the multilayers with $\Lambda=6.5$ and 9.5 nm are shown in Fig. 1. The periodic variation of the concentrations of Ti, Al, and Zr as main elements throughout the thickness gives a direct evidence of the multilayered modulation in our design. The formation of alternating ZrN and TiAlN in a nanoscale Λ is also confirmed. The elemental composition of Ti:Al = 2:1 within the TiAlN layer reflects the large difference in sputter yield of Ti and Al.

The low-angle x-ray diffraction (XRD) patterns of Fig. 2 also give the information on Λ of the ZrN/TiAlN coatings. The numerous reflection peaks as well as their narrow full width at half maximum indicate sharp interfaces between the ZrN and TiAlN layers. Their Λ are calculated to be 3.6 and 6.5 nm from the Bragg equation, which is in agreement with our estimated Λ according the deposition rate of monolithic ZrN and TiAlN coatings under identical deposition conditions.

The high-angle XRD patterns of Fig. 2 reveal that both monolithic ZrN and TiAlN coatings exhibit typical fcc struc-

^{a)}Electronic mail: dejunli@mail.tjnu.edu.cn.

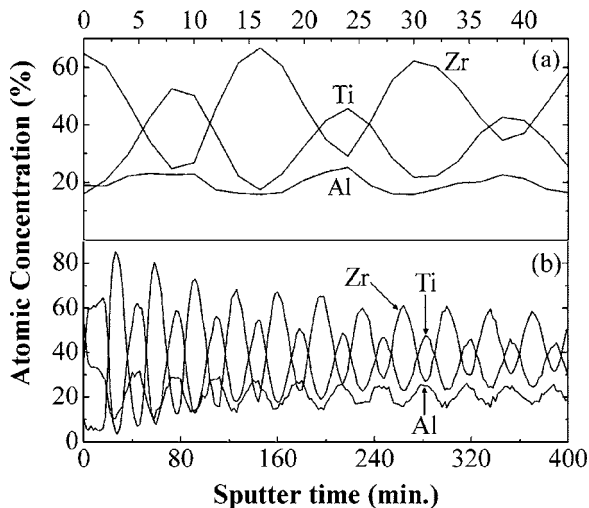


FIG. 1. Sputter depth profile of the ZrN/TiAlN coatings synthesized with (a) $\Lambda=6.5$ nm and (b) $\Lambda=9.5$ nm.

tures. The ZrN constituent layer shows strong (220) and (111) orientations. Strong TiAlN (111) as well as weak TiAlN (200), (220), and AlN (111) textures is observed in TiAlN constituent layer. The sharp ZrN (111), TiAlN (111), and AlN (111) preferred orientations are evolved in the multilayers with different Λ . We note that the ZrN (220) peak nearly disappears in the multilayered structures. It is probable that the periodic introduction of the TiAlN layer suppresses the growth of ZrN with the (220) orientation. We also note that ZrN (111) and TiAlN (111) textures become stronger with increasing Λ . This means that the growth of ZrN and TiAlN (111) grains requires a threshold Λ for proper strain optimization.

Residual stresses in our multilayers were measured and calculated according to the Stoney formula.¹² These measurements are crucial because residual stress affects industrial applications of coatings. It is well known that high residual stress is the main reason of coating delamination and plastic deformation. Figure 3 indicates that all multilayers have lower residual stress, i.e., compressive stress, than the

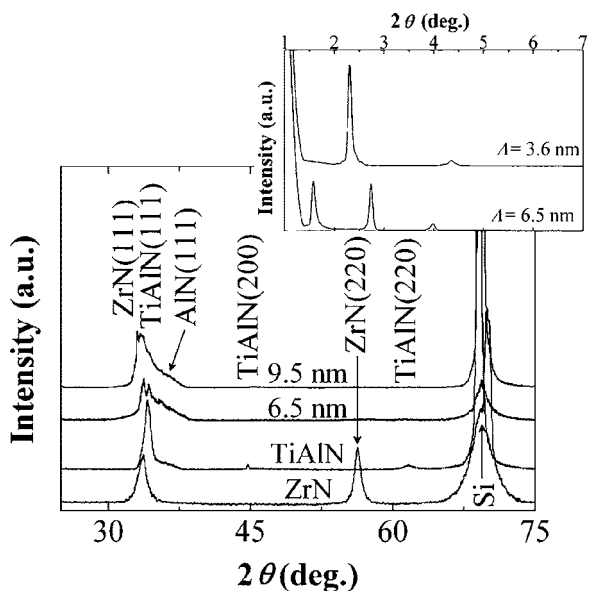


FIG. 2. Low-angle and high-angle XRD patterns for ZrN/TiAlN coatings with different Λ .

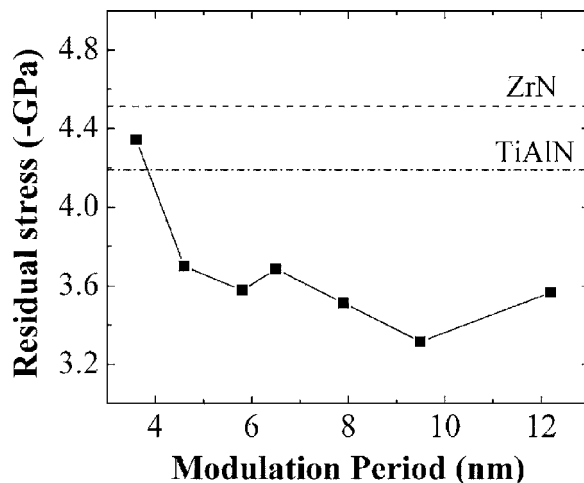


FIG. 3. Residual stress of the ZrN/TiAlN coatings vs Λ .

rule-of-mixture value of monolithic coatings. The multilayer with $\Lambda=9.5$ nm has the lowest value (-3.3 GPa). The periodic mixture of ZrN and TiAlN layers suppresses the grain growth in the constituent layers, which releases stress build in the constituent layers.

Figure 4(a) shows the hardness and elastic modulus of ZrN/TiAlN as well as monolithic ZrN and TiAlN coatings as a function of Λ . In general, multilayers reveal higher values than the rule-of-mixture value of monolithic coatings. The respective maximum hardness and elastic modulus are 30.1 and 361 GPa for Λ of 6.5 nm. The nature of the nanoscale multilayered modulation and interfaces is critical to the hardness increase, because sharp ZrN/TiAlN interfaces can pro-

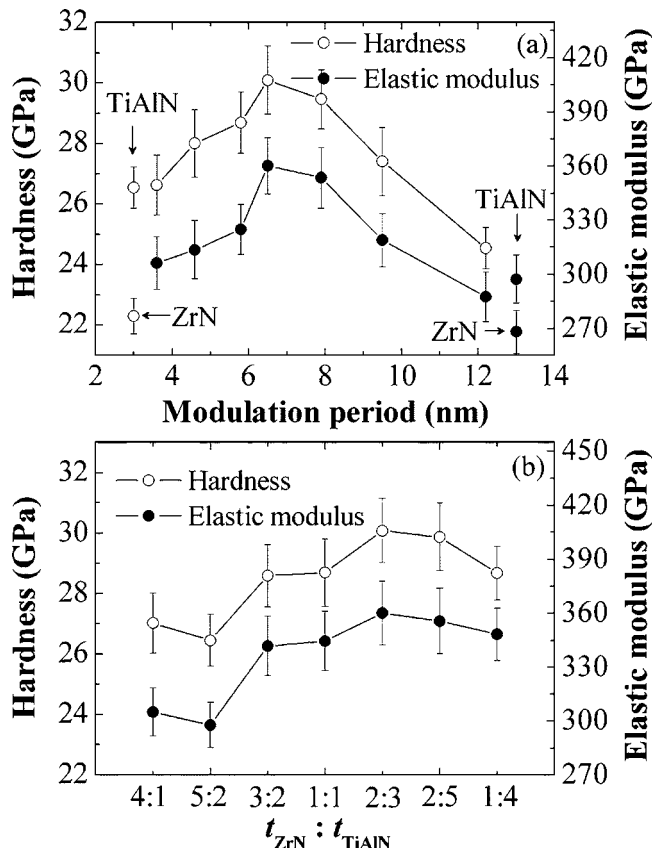


FIG. 4. Hardness and elastic modulus of the ZrN/TiAlN coatings vs (a) Λ and (b) $t_{ZrN}:t_{TiAlN}$.

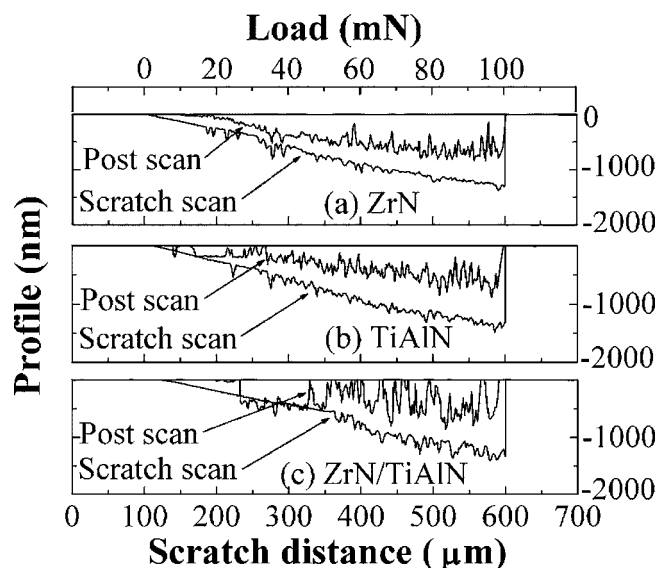


FIG. 5. Surface profiles of the scratch scan and postscan on the three different coatings.

duce barriers to dislocation glide and columnar grain growth across layers. Further, the dislocation blocking due to coherency strains for different nanocrystalline grains also makes a contribution to hardness enhancement. Besides, a strong mixture of ZrN (111), TiAlN (111), and AlN (111) textures also leads to high hardness and modulus.

The effect of $t_{\text{ZrN}}:t_{\text{TiAlN}}$ on hardness and elastic modulus for the multilayers with a Λ of 6.5 nm is also showed in Fig. 4(b). The maximum hardness is over 30 GPa when $t_{\text{ZrN}}:t_{\text{TiAlN}}$ is 2:3. So, proper modulation ratio can produce synergetic strain-optimization effects on mechanical properties of the multilayers.

Figure 5 shows the scratch scan and postscan surface profiles on the monolithic ZrN, TiAlN, as well as the ZrN/TiAlN coatings with $\Lambda=6.5$ nm and $t_{\text{ZrN}}:t_{\text{TiAlN}}=2:3$. These scratch scan profiles all indicate an abrupt increase point in scratch depth. The critical fracture load (L_c) of the coating corresponding to this point characterizes the adhe-

sion strength of the coating. The L_c of monolithic ZrN and TiAlN coatings are 17.1 and 24.3 mN, respectively. However, the ZrN/TiAlN coating exhibits smooth scratch scan and postscan surface profiles. Its L_c approaches to 53.3 mN. This improved fracture resistance appears to be directly related to high hardness and strong plastic recovery of the coating with the multilayered modulation.

The influence of multilayered modulation structure on the properties of multilayer is a key factor in its practical applications. This work proves that IBAD can produce nanoscale multilayers with sharp ZrN/TiAlN interfaces. At the optimal modulation period of 6.5 nm and modulation ratios of 2:3 the multilayer shows high hardness, high fracture resistance, and low compressive stress.

The authors would like to thank the National Natural Science Foundation of China (50472026), International Collaboration Project of Tianjin Science and Technology Plan (07ZCGHHZ01500), Canadian Natural Science and Engineering Research Council, and Surface Science Western for their support of this work.

¹C. S. Chen, C. P. Liu, C. Y. A. Tsao, and H. G. Yang, *Scr. Mater.* **51**, 715 (2004).

²J. V. Ramana, S. Kumar, C. David, A. K. Ray, and V. S. Raju, *Mater. Lett.* **43**, 73 (2000).

³C. P. Liu and H. G. Yang, *Mater. Chem. Phys.* **86**, 370 (2004).

⁴S. G. Harris, E. D. Doyle, A. C. Vlasveld, J. Audy, and D. Quick, *Wear* **254**, 166 (2003).

⁵F. H. Mei, N. Shao, L. Wei, Y. S. Dong, and G. Y. Li, *Appl. Phys. Lett.* **87**, 011906 (2005).

⁶M. Hock, E. Schäffer, W. Döll, and G. Kleer, *Surf. Coat. Technol.* **163-164**, 689 (2003).

⁷D. J. Li, M. X. Wang, and J. J. Zhang, *Mater. Sci. Eng., A* **423**, 116 (2006).

⁸C. H. Hsu, M. Li. Chen, and K. L. Lai, *Mater. Sci. Eng., A* **421**, 182 (2006).

⁹D. J. Li, M. X. Wang, J. J. Zhang, and J. Yang, *J. Vac. Sci. Technol. A* **24**, 966 (2006).

¹⁰Q. Luo and P. Eh. Hovsepian, *Thin Solid Films* **497**, 203 (2006).

¹¹Y. Y. Chang, D. Y. Wang, and C. Y. Hung, *Surf. Coat. Technol.* **200**, 1702 (2005).

¹²M. Ohring, *The Materials Science of Thin Films* (Academic, New York, 1992), p. 416.